

Form factors of the hydrogen atom in excited states*

Michio Matsuzawa[†]

Argonne National Laboratory, Argonne, Illinois 60439

(Received 20 July 1973)

An exact closed expression for the form factor (and hence the generalized oscillator strength) for bound-free transitions of the hydrogen atom in highly excited states is derived by use of the Coulomb Green's function. The calculated densities of the generalized oscillator strength of the excited hydrogen atom with an initial principal quantum number $n_0 = 10$ are 10.9 (-5.0), 13.6 (-4.0), 22.7 (-3.0), 55.3 (-2.0), 96.2 (-1.0), 42.1 (0.0), and 4.63 (1.0) in Ry^{-1} near the ionization threshold [for $E/I(n_0) = 1.0001$]. Here a figure in parentheses denotes the value of $\ln(n_0^2 q^2)$, where q is the magnitude of the momentum transfer, E the excitation energy measured from the state n_0 , and $I(n_0)$ the ionization potential. Using these results, we draw the Bethe surface, i.e., a three-dimensional plot of the density of the generalized oscillator strength as a function of E and $\ln q^2$. This surface gives a quantitative understanding for the entirety of the inelastic process of this excited atom by charged particles. The validity of the binary-encounter theory is quantitatively discussed. The Born cross sections for excitations ($n_0 - n_0 + 1$, $n_0 - n_0 + 2$, $n_0 - 2n_0$ transitions) and ionization are evaluated for the case of $n_0 = 10$ and 20. Finally, an application of this form factor to the collisional ionization of the highly excited atom with a molecule is briefly mentioned.

I. INTRODUCTION

Collisions of a charged particle with an initially excited atom may result in deexcitation to a lower level, in excitation to a higher level, or in ionization. Quantitative knowledge of such collisions, particularly with an atom in highly excited states, is meager at present, while there has been an increasing demand for it from many applications, such as physics of gaseous discharges, plasma physics, astrophysics, and radiation physics.

In inelastic processes of highly excited states of an atom there are two major points different from those of the ground state, namely, (i) transition energies may be very small, and (ii) level spacings between adjacent levels are very close. Under condition (i) the first Born approximation seems to be valid even at velocities of an incident particle which are considered to be slow for collisions of an atom in the ground or lower excited states. On the other hand, condition (ii) means that states other than the initial and final ones may be important in the collision process because of their close coupling with the initial and final states. This appears to be an unfavorable condition for a two-state approximation such as the Born approximation. To my knowledge, however, there has been no clear-cut conclusion about the range of validity of the first Born approximation for the transitions between highly excited states. We do not consider this problem further.

If we restrict our discussions to the case where the first Born approximation is adequate (at least where the incident charged particle is much faster than the atomic electron to be affected in the collision),

the essential part of the calculations is that of form factors, or equivalently of generalized oscillator strengths, for pertinent transitions.

The form factor of the hydrogen atom in excited states is, of course, a very important quantity in atomic physics. Indeed, this gives a starting point for a general study of some dynamical properties of an atom or molecule in highly excited states, where effects of a nonhydrogenic core may be incorporated by use of the quantum defect theory.¹

Even for the hydrogen atom, where all eigenfunctions are known, we find only fragmentary numerical data on its form factor. The reason for this is that explicit computation of the hydrogen form factor as an integral meets formidable difficulties in actual numerical evaluation because of rapidly varying wave functions, particularly when the initial state has a high principal quantum number n_0 .

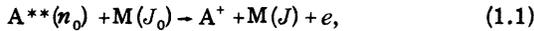
From group-theoretical considerations, Barut and Kleinert² obtained the exact form factors of the hydrogen atom between any two excited states. These expressions, however, seem to be inconvenient for numerical evaluation, especially for high n_0 . Milford and co-workers³ and later Omidvar⁴ calculated the Born cross sections for excitation of the hydrogen atoms in excited states with $n_0 \leq 7$. For higher n_0 , there have been some studies which give approximate formulas for cross sections.⁵ Recently, Beigman *et al.*⁶ derived an exact closed expression for the form factor for bound-bound transitions of the hydrogen atom in excited states summed over initial (l_0, m_0) and final (l, m) substates, which is convenient for numerical computation. These authors, however,

gave little numerical results.

As for the ionization of the hydrogen atom in the excited states by electron impact, Omidvar^{7,8} calculated the Born cross sections for all partial waves with $n_0 \leq 5$ and for a limited number of sub-states with $6 \leq n_0 \leq 10$. There has been, however, no calculation for ionization of the hydrogen atom in excited states with higher n_0 except for some approximate treatments.⁹ Practically no data on the angular distribution (or the form factor itself) for excitation and ionization are found in the literature.

The major purposes of the present paper are as follows: (i) to derive an exact closed expression of the form factors for bound-free transitions of excited hydrogen atoms; (ii) to present extensive numerical results (in the form of a contour map of the Bethe surface¹⁰) for excitation and ionization of the hydrogen atom in excited states, including information on the angular distribution of a scattered electron; and (iii) to assess the validity of the binary-encounter theory for these excited states quantitatively.

Another motivation of the present work stems from a theory of the collisional ionization of a highly excited noble-gas atom A^{**} with a polar molecule given by the present author.¹¹ At room temperature, the molecule is likely to be in a rotationally excited state. An electron in a high Rydberg state becomes ionized by energy gain from the deexcitation of the rotationally excited polar molecule, namely,



where J_0 and J are the rotational quantum numbers of the polar molecule for initial and final states, respectively. Within the hydrogenic approximation to the highly excited noble-gas atom, the cross section for process (1.1) can be expressed in terms of the form factor or the generalized oscillator strength for the hydrogen atom in highly excited states. The detailed treatment of process (1.1) using the results of the present calculation will be published elsewhere.

II. DENSITIES OF THE FORM FACTORS FOR BOUND-FREE TRANSITIONS OF THE HYDROGEN ATOM IN EXCITED STATES

Within the Born approximation, the differential ionization cross section $d\sigma_{n_0}/dE$ of excited hydrogen atoms with n_0 by electron impact per unit range of excitation energy can be expressed in terms of the density of the form factor $dF_{n_0}(q, E)/dE$, namely,

$$\frac{d\sigma_{n_0}}{dE} = \frac{8\pi}{k_i^2} \int_{|k_i - k_f|}^{k_i + k_f} \frac{dF_{n_0}(q, E)}{dE} \frac{dq}{q^3} \quad (2.1)$$

and

$$\frac{dF_{n_0}(q, E)}{dE} = n_0^{-2} \int d\Omega \sum_{l_0 m_0} |\langle E\Omega^- | e^{i\vec{q}\cdot\vec{r}} | n_0 l_0 m_0 \rangle|^2, \quad (2.2)$$

where E is the excitation energy of the ionization process measured from the initial state, Ω is the direction of the ejected electron, l_0 and m_0 are the orbital angular momentum and the magnetic quantum number of the initial state, respectively, \vec{k}_i and \vec{k}_f are the wave vectors of an incident electron and a scattered one, respectively, and \vec{q} is the momentum transfer. [Atomic units ($m = e = \hbar = 1$), together with the rydberg as the unit of energy, are used unless otherwise stated.] The final continuum state is normalized as follows:

$$\langle E\Omega^+ | E\Omega'^+ \rangle = \delta(E - E') \delta(\Omega - \Omega'),$$

where the plus and minus denote the boundary conditions for an outgoing wave and an incoming wave for the ejected electron, respectively. Here we must take the ingoing-wave boundary condition¹² in the final continuum state in Eq. (2.2).

If the density of generalized oscillator strength per unit range of energy $df_{n_0}(q, E)/dE$ is used, the differential cross section $d\sigma_{n_0}/dE$ has the form

$$\frac{d\sigma_{n_0}}{dE} = \frac{4\pi}{k_i^2} \int_{n_0^2 q_{\min}^2}^{n_0^2 q_{\max}^2} \frac{1}{E} \frac{df_{n_0}(q, E)}{dE} d\ln[(n_0 q)^2], \quad (2.3)$$

where

$$\frac{df_{n_0}(q, E)}{dE} = \left(\frac{E}{q^2}\right) \frac{dF_{n_0}(q, E)}{dE}, \quad (2.4)$$

$$q_{\min} = |k_i - k_f|, \quad q_{\max} = k_i + k_f,$$

and

$$k_i^2 = k_f^2 + E.$$

In order to evaluate the squared matrix element of $e^{i\vec{q}\cdot\vec{r}}$ summed over (l_0, m_0) and integrated over Ω , we use the spectral representation of the Coulomb Green function $G_W(\vec{r}, \vec{r}')$,

$$G_{W \pm i\epsilon}(\vec{r}, \vec{r}') = \sum_{nlm} \frac{|nlm\rangle \langle nlm|}{W - W_n} + \iint dW' d\Omega \frac{|E'\Omega^+\rangle \langle E'\Omega^+|}{W \pm i\epsilon - W'} \quad \text{with } \epsilon > 0, \quad (2.5)$$

similarly to the procedure in Ref. 6, where $W_n (= -1/n^2)$ and W' are the eigenvalues of Hamiltonian of the hydrogen atom. Here we have the re-

lation $E' = W' - W_{n_0}$. We can relate the squared matrix element of $e^{i\vec{q}\cdot\vec{r}}$ summed over l_0, m_0 and integrated over Ω to the gap of the Coulomb Green function at a branch cut of a real positive W . As shown in the Appendix, we get

$$\begin{aligned} & \sum_{l_0 m_0} \int d\Omega |\langle E\Omega^- | e^{i\vec{q}\cdot\vec{r}} | n_0 l_0 m_0 \rangle|^2 \\ &= \sum_{l_0 m_0} \int d\Omega |\langle E\Omega^+ | e^{i\vec{q}\cdot\vec{r}} | n_0 l_0 m_0 \rangle|^2 \\ &= \mp \pi^{-1} \lim_{W' \rightarrow W_{n_0}} (W' - W_{n_0}) \int G_{W'}(\vec{r}, \vec{r}') \\ & \quad \times e^{-i\vec{q}\cdot(\vec{r}-\vec{r}')} \text{Im} G_{W \pm i\epsilon}(\vec{r}', \vec{r}) d\vec{r}' d\vec{r}'. \quad (2.6) \end{aligned}$$

Integration over Ω gives the same result for both the boundary condition of the ingoing wave and that of the outgoing wave. (For obtaining the correct angular distribution for the ejected electron, we must use the incoming-wave boundary condition.) The Coulomb Green function in configurational space has the closed form¹³

$$\begin{aligned} G_W(\vec{r}, \vec{r}') &= -\Gamma(1-i/k) [2\pi i(x-y)k]^{-1} \\ & \quad \times \hat{L}[W_{i/k, 1/2}(-ikx)M_{i/k, 1/2}(-iky)], \quad (2.7) \end{aligned}$$

where

$$\begin{aligned} -\pi^{-1} \text{Im} G_{W \pm i\epsilon} &= -[4\pi^2(x-y)]^{-1} \hat{L}\{[\Gamma(1-i/k_+)/k_+] W_{i/k_+, 1/2}(-ik_+x) M_{i/k_+, 1/2}(-ik_+y) \\ & \quad - [\Gamma(1-i/k_-)/k_-] W_{i/k_-, 1/2}(-ik_-x) M_{i/k_-, 1/2}(-ik_-y)\}, \end{aligned}$$

where

$$k_{\pm}^2 = W \pm i\epsilon, \quad \epsilon > 0, \quad \arg W = 0.$$

The condition (2.8) gives a unique relation between k_+ and k_- , namely,

$$\begin{aligned} \lim_{\epsilon \rightarrow +0} k_- &= e^{i\pi} \lim_{\epsilon \rightarrow +0} k_+, \\ \lim_{\epsilon \rightarrow +0} \arg k_+ &= 0. \quad (2.11) \end{aligned}$$

This ensures that the domain of the Coulomb Green function is limited to the first "physical" sheet in a complex W plane. Using Eq. (2.11) and properties of the Whittaker function,¹⁵ we can obtain Eq. (2.10), where we have put

$$k = \lim_{\epsilon \rightarrow +0} k_+(\epsilon).$$

Laurenzi¹⁶ calculated the same quantity. However, his result seems to be incorrect. (Apparently that result stems from a confusion as to the choice of the appropriate branch of the Coulomb Green function.)

Substitution of Eqs. (2.9) and (2.10) into (2.2)

$$k^2 = W, \quad \text{Im} k > 0, \quad (2.8)$$

$$\hat{L} = \frac{\partial}{\partial x} - \frac{\partial}{\partial y}, \quad x = r+r' + |\vec{r}-\vec{r}'|, \quad y = r+r' - |\vec{r}-\vec{r}'|,$$

and $W_{i/k, 1/2}$ and $M_{i/k, 1/2}$ are the Whittaker functions.¹⁴

The limiting process of Eq. (2.6) leads to the calculation of a residue of a pole of $G_W(\vec{r}, \vec{r}')$ for a real negative value W and of a gap of $G_W(\vec{r}, \vec{r}')$ at a branch cut for a real positive W , namely, we have

$$\lim_{W' \rightarrow W_{n_0}} (W' - W_{n_0}) G_{W'}(\vec{r}, \vec{r}') = -[n_0 \pi (x-y)]^{-1} P_{n_0} \quad (2.9)$$

and

$$\begin{aligned} -\pi^{-1} \lim_{\epsilon \rightarrow +0} G_{W \pm i\epsilon}(\vec{r}, \vec{r}') &= (2\pi k^2)^{-1} (1 - e^{-2\pi/k})^{-1} \\ & \quad \times (x-y)^{-1} P_{i/k}, \quad (2.10) \end{aligned}$$

where

$$P_\lambda = \hat{L}[M_{\lambda, 1/2}(x/\lambda)M_{\lambda, 1/2}(y/\lambda)].$$

The former relation can easily be obtained from the calculation of the residue of the Γ function as shown in Ref. 6. In order to derive Eq. (2.10) we use the closed form of the Coulomb Green function, and write

yields

$$\begin{aligned} \frac{dF_{n_0}(q, E)}{dE} &= -(2\pi^2 n_0^3 k^2)^{-1} (1 - e^{-2\pi/k})^{-1} \\ & \quad \times \int \int e^{-i\vec{q}\cdot(\vec{r}-\vec{r}')} (x-y)^{-2} P_{n_0} P_{i/k} d\vec{r}' d\vec{r}'. \quad (2.12) \end{aligned}$$

Holt¹⁷ has pointed out that the form factor $F_{n_0^n}(q)$ for excitation to the final bound state with n can be obtained as

$$F_{n_0^n}(q) = -2\pi i \left[\text{residue of } \frac{dF_{n_0}(q, k)}{dk} \text{ at } k = \frac{i}{n} \right]. \quad (2.13)$$

Using the expression of Eq. (2.12) and relation $dF_{n_0}(q, k)/dk = 2kdF_{n_0}(q, E)/dE$, we can easily get

$$\begin{aligned} F_{n_0^n}(q) &= \pi^{-2} n_0^{-3} n^{-1} \int e^{-i\vec{q}\cdot(\vec{r}-\vec{r}')} (x-y)^{-2} \\ & \quad \times P_{n_0} P_n d\vec{r}' d\vec{r}'. \quad (2.14) \end{aligned}$$

This is equivalent to the result of Ref. 6, which corroborates the correctness of Eq. (2.12). The

right-hand side of Eq. (2.12) can be calculated in a way similar to Ref. 6. Therefore, we give below only the final result,¹⁸

$$A_i(q) = (96 n_0 k^2)^{-1} (1 - e^{-2\pi/k})^{-1} \int_0^\infty \int_0^\infty e^{-iq(x-y)/2} (x^2 + 4xy + y^2) P_{n_0} P_{i/k} dx dy. \quad (2.16)$$

The last integral can be written in terms of hypergeometric functions as follows:

$$A_i(q) = (2n_0^2 k)^{-1} [1 - e^{-2\pi/k}]^{-1} \text{Im} \left\{ [I'_\mu(-n_0 + 1, -i/k + 1) I'_\mu(-n_0, -i/k + 1)^* - I'_\mu(-n_0 + 1, -i/k) I'_\mu(-n_0, -i/k)^*] \right. \\ \left. - \frac{1}{8} \frac{\partial^2}{\partial q^2} [I_\mu(-n_0 + 1, -i/k + 1) I_\mu(-n_0, -i/k + 1)^* - I_\mu(-n_0 + 1, -i/k) I_\mu(-n_0, -i/k)^*] \right\}. \quad (2.17)$$

Here $I_\mu(\alpha, \alpha')$ is given by

$$I_\mu(\alpha, \alpha') = \int_0^\infty e^{-\mu x} F(\alpha, 1; p x) F(\alpha', 1; p' x) dx \\ = \mu^{\alpha+\alpha'} (\mu - p)^{-\alpha} (\mu - p')^{-\alpha'} F(\alpha, \alpha', 1; \xi), \quad (2.18)$$

where

$$p = 1/n, \quad p' = -ik, \quad \mu = (p + p' + iq)/2,$$

$$\xi = p p' (\mu - p)^{-1} (\mu - p')^{-1}, \quad \text{and } I' = \frac{\partial I}{\partial q}.$$

III. RESULTS AND DISCUSSION

A. Density of the generalized oscillator strength and the Bethe surface

Numerical values of $F_{n_0 n}(q)$ and $dF_n(q, E)/dE$ can be obtained from expressions (2.15), (2.17), and (2.18), together with the results of Ref. 6. Numerical integrations are done by means of the Simpson quadrature. Our coded program is numerically checked by available data for the cases of excitation and ionization for $n_0 = 1$ (Ref. 19), $n_0 = 2$ (Ref. 17), and $n_0 = 5$ (Refs. 4 and 8), and for the optical oscillator strength $f_{n_0 n}(0)$ for $n_0 \leq 14$ (Ref. 20). Up to $n_0 = 20$, this program can give us accurate results for almost all final states except for extremely high n and for a very low energy W of the ejected electron. For example, for the case $n_0 = 25$, our program does not work for transitions for $|n_0 - n| = 1$ because of underflow and overflow in the course of numerical computation (in our computer, the magnitude of a real constant is limited to the range between 10^{-78} and 10^{75}), but gives accurate results for almost all other transitions.

The generalized oscillator strength is a quantity which is suitable for the understanding of the inelastic scattering of an atom by charged particles. Typical numerical results for $df_{n_0}(q, E)/dE$

$$\frac{dF_{n_0}(q, E)}{dE} = -n_0^{-2} q^{-1} \int_0^q A_i(q) dq \quad (2.15)$$

and

are shown for the cases of $n_0 = 10$ and 20 in Figs. 1 and 2.²¹ In these figures, for the case of excitation and deexcitation, we plot the quantities $f_{n_0 n}(q)(n^3/2)$ instead of $f_{n_0 n}(q)$. One can see that the continuity relation²²

$$\lim_{n \rightarrow \infty} f_{n_0 n}(q)(n^3/2) = \left. \frac{df_{n_0}(q, E)}{dE} \right|_{E=I(n_0)} \quad (3.1)$$

is numerically satisfied where $I(n_0)$ is the ionization potential of the initial state, namely, $I(n_0) = |W_{n_0}|$. To test the consistency of these numerical values of $f_{n_0 n}(q)$ and $df_{n_0}(q, E)/dE$, we have calculated the sum $S(q)$ of the generalized oscillator strength,

$$S(q) = \sum_{n=1}^{\infty} f_{n_0 n}(q) + \int_{I(n_0)}^{\infty} \left(\frac{df_{n_0}(q, E)}{dE} \right) dE, \quad (3.2)$$

which must be equal to unity according to the Bethe sum rule.¹⁹ Table I shows a typical example in which the Bethe sum rule is satisfied within 1% for $n_0 = 10$.

The Bethe surface,^{10, 23} namely, a three-dimensional plot of $df_{n_0}(q, E)/dE$ as a function of $E/I(n_0)$ and $\ln(n_0^2 q^2)$, can be drawn using the calculated results of $f_{n_0 n}(q)$ and $df_{n_0}(q, E)/dE$. Figure 3 shows a contour map of the Bethe surface for $n_0 = 10$. This figure gives a comprehensive picture of the inelastic scattering.

In the Bethe surface of the hydrogen atom in excited states, there appear some new features that are distinct from the surface of the ground state,²³ namely, (i) the emergence of a negative-valued region corresponding to deexcitation, (ii) an extreme concentration of $df_{n_0}(q, E)/dE$ on a very small $E/I(n_0)$ for a small $(n_0 q)^2$ (note that the scale of contours in Fig. 3 is logarithmic), (iii) the conspicuous appearance of the Bethe ridge for lower E , and (iv) the appearance of a fine structure in $df_{n_0}(q, E)/dE$. A commentary will be made below on each of these points.

Because of point (i), the generalized oscillator strength $f_{n_0 n}(q)$ can exceed unity for some n , a property which cannot occur for the ground state because of the Bethe sum rule.

Point (ii) means that there are a very limited number of bound-bound transitions in which soft collisions, i.e., small-angle scatterings, are important. In bound-bound transitions, where the binding of the electron is strong in the final state, namely, deexcitation to the final state with $n \approx 1$,

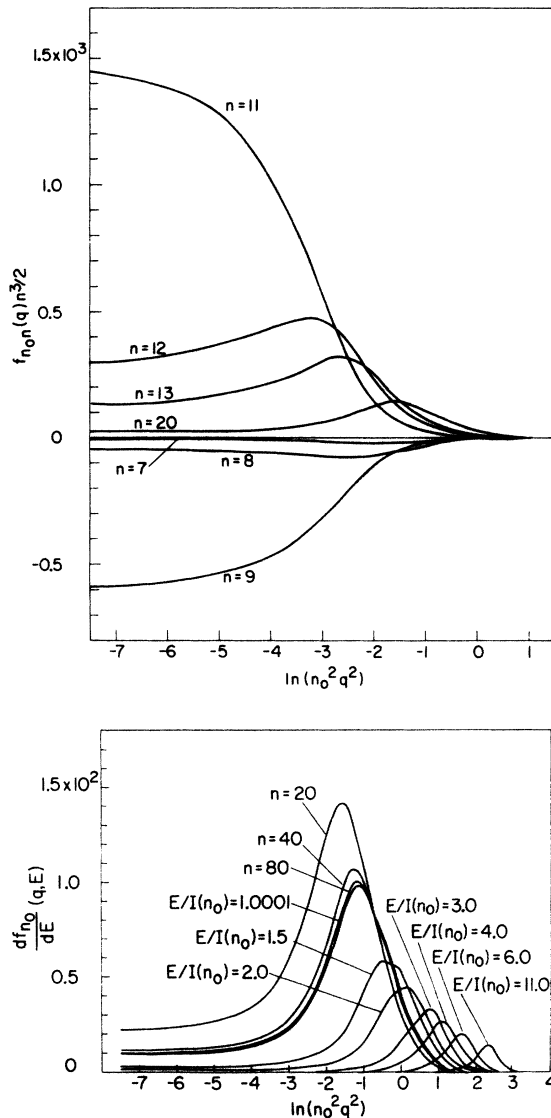


FIG. 1. Densities of the generalized oscillator strength $df_{n_0}(q, E)/dE$ for the hydrogen atom with $n_0 = 10$. For the cases of excitation or deexcitation $f_{n_0 n}(q) n^{3/2}$ is plotted. The notation n is the principal quantum number of the final discrete state, and $E/I(n_0)$ represents the excitation energy in units of the ionization potential of the initial state.

soft collisions are also important. In these two types of bound-bound transitions, the dipole property plays an important role. However, the latter type transitions occur only with a very small probability.

For high-energy transfer E and high $(n_0^2 q^2)$, the Bethe ridge is common to all atoms and molecules. Hence, point (iii) states that the hydrogen atom loses its own character and the bound electron behaves more and more like a free one as it becomes more and more highly excited. Further, for the case of deexcitation, there should occur the situation similar to the case of excitation if

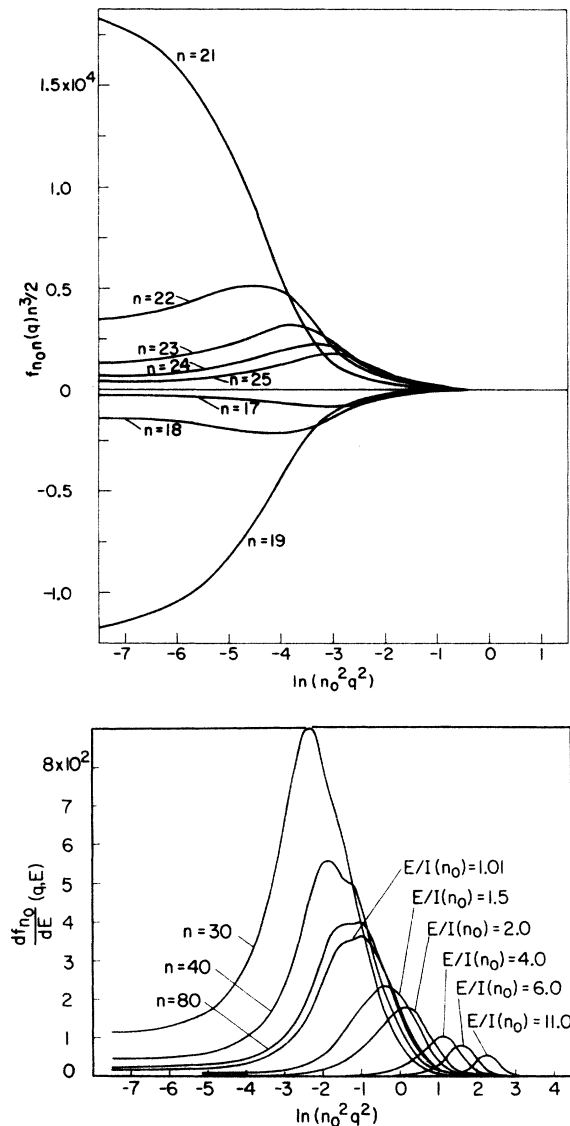


FIG. 2. Densities of the generalized oscillator strength $df_{n_0}(q, E)/dE$ for the hydrogen atom with $n_0 = 20$. As for notations n and $E/I(n_0)$, see the caption to Fig. 1.

the conditions

$$|n-n_0| \gg 1, n \gg 1, n_0 \gg 1 \quad (3.3)$$

are satisfied. In this case, we have a "valley" along the trajectory which is determined by the relation $q^2 = |E|$ in the negative-valued region of the Bethe surface. This valley dies out in the region where the binding of the bound electron in the final state becomes strong. We shall discuss this point in further detail.

In the region where the Bethe ridge appears conspicuously, the binary-encounter theory is likely to be valid.^{24,25} There have been many studies on inelastic processes of the hydrogen atom in excited states by impact of charged particles based on the binary-encounter theory.²⁶ So far, we have found only qualitative discussions about the validity of this theory to highly excited states.²⁷ According to the binary-encounter theory, the density of the generalized oscillator strength is written as

$$\frac{df_{n_0}^{\sim}(q, E)}{dE} = \frac{2^3 E}{3\pi n_0^5} \frac{q^3}{[(q^2 - E)^2 + 4q^2/n_0^2]^3}, \quad (3.4)$$

where use has been made of the momentum distribution of excited hydrogen atoms with n_0 averaged over l_0, m_0 obtained by Fock.²⁸ For the bound-bound transitions $df_{n_0}^{\sim}(q, E)/dE$ should be interpreted as $f_{n_0 n}(q)(n^3/2)$. Further, E should be taken to be $E(n_0, n) = W_n - W_{n_0}$. Figure 4 shows a contour map of the relative difference between $df_{n_0}^{\sim}(q, E)/dE$ and the correct one for $n_0 = 10$. The generalized oscillator strength $df_{n_0}^{\sim}(q, E)/dE$ agrees well with the correct one along the Bethe ridge and in the region II [and along the valley in the negative-valued region, if the conditions (3.3)

are satisfied]. In region I, this theory fails to express soft collisions with small $\ln(n_0^2 q^2)$. One can quantitatively see how the extent of the agreement of Eq. (3.4) with the correct one changes in the transition region from the Bethe ridge to region I. Figure 5 shows the dependence of the contour of 10% relative difference between Eq. (3.4) and the correct one on n_0 . This figure immediately indicates the widening of the region where the binary-encounter theory is valid on the $\ln(n_0^2 q^2) - E/I(n_0)$ plane, which originates from the looser binding of an electron with higher n_0 . Further, this figure enables us to assess the validity of the binary-encounter theory or of the impulse approximation applied to various problems.

Point (iv), namely, the fine structure, appears in $df_{n_0}^{\sim}(q, E)/dE$ for higher excited states at E

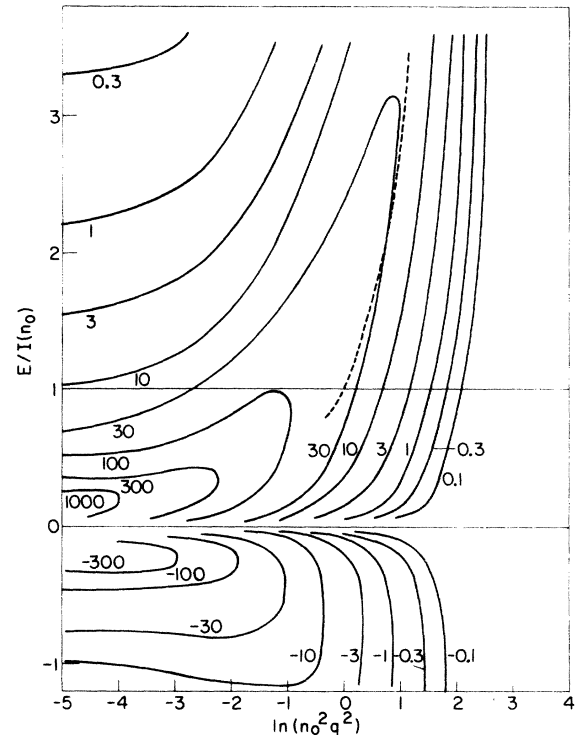


FIG. 3. Contour map of the Bethe surface for the hydrogen atom with $n_0 = 10$. The regions $E/I(n_0) \geq 1$, $1 > E/I(n_0) > 0$, and $0 > E/I(n_0)$ represent ionization, excitation, and deexcitation, respectively. Figures attached to each contour denote the value of $df_{n_0}^{\sim}(q, E)/dE$ or $f_{n_0 n}(q)(n^3/2)$. In the regions of excitation and deexcitation the contour lines are drawn by the smooth connection of discrete points. This figure shows the main portion of the surface, namely, $-5 \leq \ln(n_0^2 q^2) \leq 4$, and $-1.2 < E/I(n_0) < 3.6$. The dotted line shows the location $n_0^2 q^2 = E/I(n_0)$ of the Bethe ridge. Note that the Bethe ridge is a universal curve on the $\ln(n_0^2 q^2) - E/I(n_0)$ plane.

TABLE I. Test of the Bethe sum rule for the 10th excited state.

$\ln(n_0^2 q^2)$	-5.0	-2.5	0.0
$\sum_{n=1}^{n_0-1} f_{n_0 n}(q)$	-1.757	-0.962	-0.113
$\sum_{n=n_0+1}^{\infty} f_{n_0 n}(q)^a$	2.704	1.834	0.189
$\int_{I(10)}^{\infty} \left(\frac{df_{n_0}^{\sim}(q, E)}{dE} \right) dE$	0.057	0.128	0.928
$S(q)$	1.004	1.000	1.004

^aThe quantities in the third row have been calculated by the following approximate formula:

$$\sum_{n=n_0+1}^{\infty} f_{10n}(q) \approx \sum_{n=11}^{19} f_{10n}(q) + \frac{1}{2} f_{10, 20}(q) + \int_{E(10, 20)}^{I(10)} f_{10n}(q)(n^3/2) dE.$$

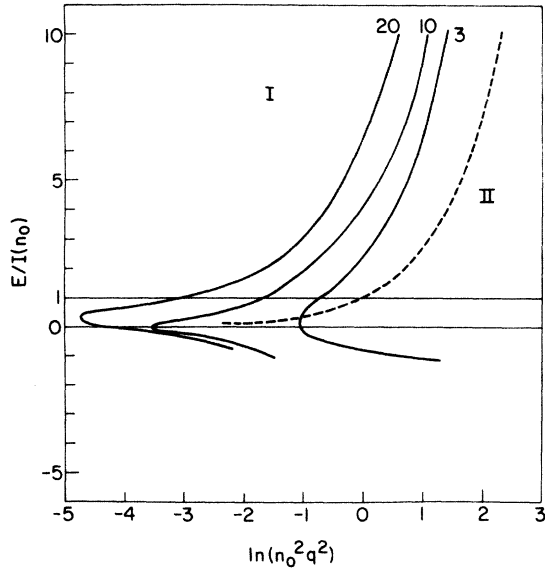


FIG. 4. Comparison with the binary-encounter theory for the densities of the generalized oscillator strength of the hydrogen atom with $n_0=10$. Each line represents the contour. Figure attached to each line denotes relative difference between the binary-encounter theory and the correct one in percentage. The dotted line shows the location of the Bethe ridge. Note that the value on the straight line, $E=0$, has no meaning for the densities of the generalized oscillator strength.

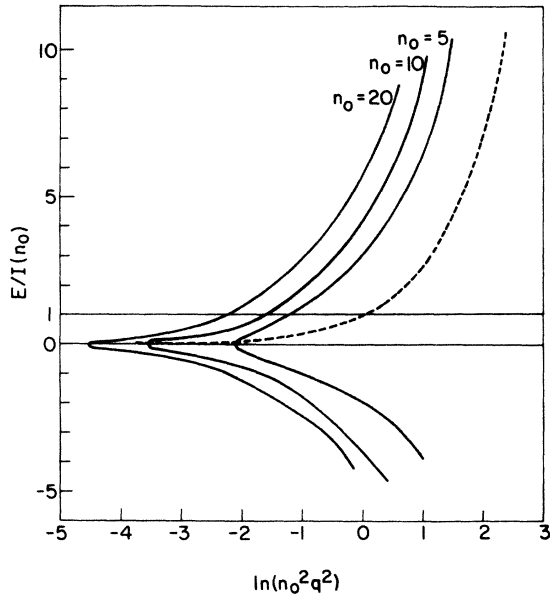


FIG. 5. Dependence of contour of 10% relative difference between the binary-encounter theory and the correct one for the densities of the generalized oscillator strength on n_0 . Figure attached to each contour denotes the principal quantum number n_0 of the highly excited state. See also caption to Fig. 4.

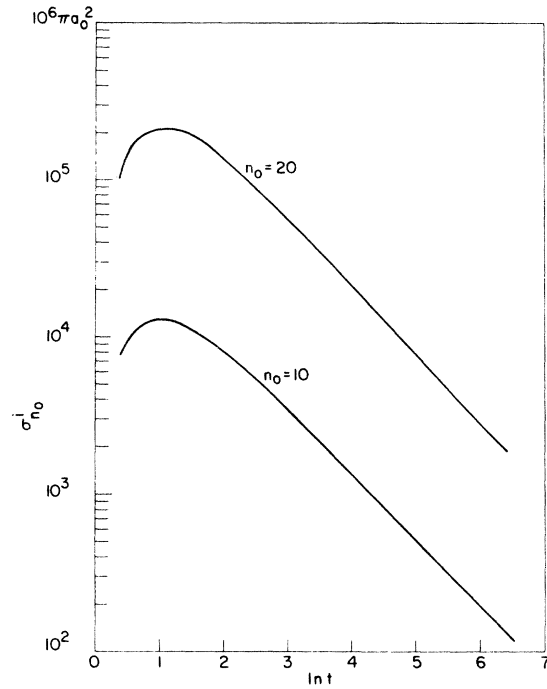


FIG. 6. Born ionization cross sections for the n_0 th highly excited hydrogen atom. Here t stands for $T/I(n_0)$.

$\approx I(n_0)$. For the generalized oscillator strengths for ionization of the hydrogen atom in the 2s and 3s excited states, Nikolaev and Kruglova²⁹ found some minima which can be related to the nodes of the momentum-space wave function. However, after averaging over initial substates, these minima vanish. Unfortunately, our method cannot give us the generalized oscillator strength for each initial and final substate. At present, it is not understood which combinations of initial and final states are responsible for the fine structure.

B. Born cross sections for ionization and excitation

Using Eq. (2.3), total ionization can be easily obtained after the integration over E , namely,

$$\sigma_{n_0}^i = \int_{I(n_0)}^T \left(\frac{d\sigma_{n_0}}{dE} \right) dE,$$

where T is the kinetic energy of an incident electron. For the case of $n_0=5$, our calculated results are found to agree with those of Omidvar⁸ within a few percent. The ionization cross sections for the excited states with $n_0=10$ and 20 are given in Fig. 6. In order to calculate the Born excitation cross section $\sigma_{n_0 n'}$, one has only to replace $df_n(q, E)/dE$ by $f_{n_0 n}(q)$ and E by $E(n, n')$ in formula (2.3). For the case where $n_0=5$, our calculated results agree well with those of Omid-

var.⁴ Calculated excitation cross sections for $n_0 \rightarrow n_0 + 1$ transitions are shown in Fig. 7.

For sufficiently high velocity, as pointed out by Fano,³⁰ a plot of $t\sigma$ vs $\ln t$ becomes a straight line, namely,

$$t\sigma = a \ln t + b \quad (\sigma \text{ in } \pi a_0^2), \quad (3.5)$$

where $t = T/E(n_0, n)$ for excitation, and $t = T/I(n_0)$ for ionization. The values of a and b in the Bethe asymptotic formula obtained by fitting the calculated results to Eq. (3.5) are shown in Tables II and III for $n_0 \rightarrow n_0 + 1$, $n_0 \rightarrow n_0 + 2$, and $n_0 \rightarrow 2n_0$ excitation and ionization. For the transitions with small E , the first term in the right-hand side of Eq. (3.5) plays a dominant role, which means that the dipole property of the hydrogen atom in excited states governs this inelastic process. As E becomes larger, the second term of the right-hand side in Eq. (3.5) becomes more important, and the region where the asymptotic formula (3.5) is valid shifts to the higher-incident-energy region. One can qualitatively understand these trends from Tables II and III.

There have been some approximate evaluations of a and b in Eq. (3.5) for $n_0 \rightarrow n_0 + 1$ and $n_0 \rightarrow n_0 + 2$, given by Saraph^{5(a)} and by Kingston *et al.*^{5(c),5(d)} Comparisons of these results with the present calculations are given in Table IV. As for the

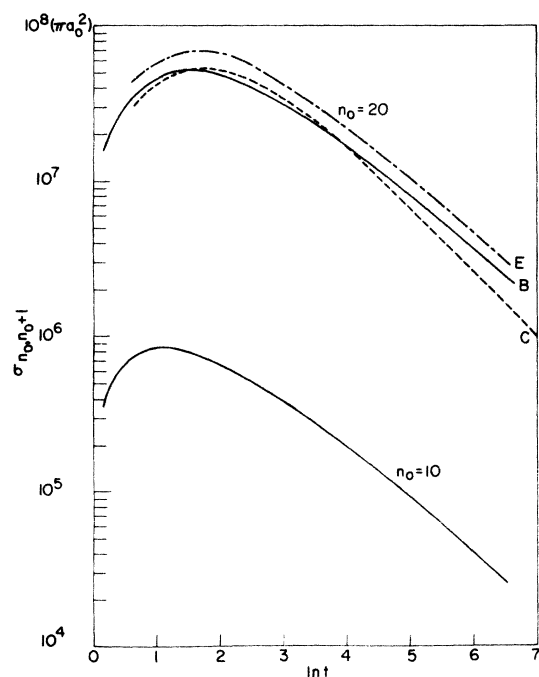


FIG. 7. Born excitation cross sections for $n_0 \rightarrow n_0 + 1$ transitions. t stands for $T/E(n_0, n)$, B is the present Born result, E is Johnson's formula (Ref. 31), and C is the classical treatment by Flannery [Ref. 26(a)].

TABLE II. The values of parameters in the asymptotic formula for $n_0 = 10$.

	Excitation			Ionization
	10 → 11	10 → 12	10 → 20	
a	2.86×10^6	1.55×10^5	3.85×10^2	1.93×10^3
b	-0.76×10^6	3.20×10^5	5.45×10^3	6.52×10^4

parameter a , these values agree with our values within a few percent; on the other hand, the parameters b from their work, especially those by Saraph, are not in agreement with ours. These numerical discrepancies may have come from the procedure of extrapolating the values of b for lower n_0 ($n_0 \leq 5$) into higher n_0 used by them.

Johnson³¹ measured the population densities of neutral helium in plasmas and adjusted a parameter in an assumed cross-section formula for transitions between highly excited states of helium from this measurement. This formula may be applied to a highly excited H atom. For $n_0 \rightarrow n_0 + 1$ transitions, the values given by Johnson, together with those based on the classical treatment by Flannery,^{26(a)} are also shown in Fig. 7. In the high-energy region where the Born approximation is adequate, our result agrees better with that of Johnson than the classical treatment. However, even within this region, there is a definite discrepancy between Johnson's and our data. This is due to the fact that he used the assumed form of the cross-section formula to reproduce Saraph's result^{5(a)} for $n_0 \rightarrow n_0 + 1$ transitions in the high-energy region.

Our approach gives only the squared matrix elements of $e^{i\vec{q}\cdot\vec{r}}$ summed over (l_0, m_0) and integrated over Ω or summed over (l, m) . Hence, from our results, one cannot get any information on each initial (n_0, l_0, m_0) or final (n, l, m) and on the angular distribution of the ejected electron for higher n_0 , which remains to deserve further detailed quantitative evaluation.

ACKNOWLEDGMENTS

I wish to express my cordial thanks to Dr. Mitio Inokuti for his valuable comments and his helpful discussions during the course of this work, and

TABLE III. The values of parameters in the asymptotic formula for $n_0 = 20$.

	Excitation			Ionization
	20 → 21	20 → 22	20 → 40	
a	3.01×10^8	1.32×10^7	1.70×10^3	1.51×10^4
b	-2.89×10^8	2.44×10^7	4.68×10^4	1.09×10^6

TABLE IV. Comparison of the parameters a and b with those from other work.

$n_0 \rightarrow n_0 + 1$ excitation						
	Present	$n_0=10$ Ref. 5 (a)	Ref. 5 (c)	Present	$n_0=20$ Ref. 5 (a)	Ref. 5 (c)
a	2.86×10^6	2.91×10^6	2.91×10^6	3.01×10^8	3.05×10^8	3.04×10^8
b	-0.76×10^6	-4.91×10^6	-1.06×10^6	-2.89×10^8	-7.46×10^8	-3.12×10^8
$n_0 \rightarrow n_0 + 2$ excitation						
	Present	$n_0=10$ Ref. 5 (d)		Present	$n_0=20$ Ref. 5 (d)	
a	1.55×10^5	1.46×10^5		1.32×10^7	1.29×10^7	
b	3.20×10^5	3.76×10^5		2.44×10^7	2.85×10^7	

for his critical reading of the manuscript. I also wish to thank Dr. Y.-K. Kim for his critical reading of the manuscript.

APPENDIX

In the first place, we consider the following quantities:

$$I_{\pm}(\vec{q}) = \sum_{l_0 m_0} \langle n_0 l_0 m_0 | e^{i\vec{q} \cdot \vec{r}} G_{W \pm i\epsilon}(\vec{r}, \vec{r}') \times e^{i\vec{q} \cdot \vec{r}'} | n_0 l_0 m_0 \rangle. \quad (\text{A1})$$

Substitution of the spectral representation of the Green function (2.5) into (A1) yields

$$I_{\pm}(\vec{q}) = \sum_{l_0 m_0} \sum_{lm} \frac{|\langle nlm | e^{i\vec{q} \cdot \vec{r}} | n_0 l_0 m_0 \rangle|^2}{W - W_n} + \sum_{l_0 m_0} \int dW' \int d\Omega \frac{|\langle E'\Omega \pm | e^{i\vec{q} \cdot \vec{r}} | n_0 l_0 m_0 \rangle|^2}{W \pm i\epsilon - W'}. \quad (\text{A2})$$

Then we obtain

$$\text{Im}_{\epsilon \rightarrow +0} I_{\pm}(\vec{q}) = \mp \pi \sum_{l_0 m_0} \int d\Omega |\langle E\Omega \pm | e^{i\vec{q} \cdot \vec{r}} | n_0 l_0 m_0 \rangle|^2, \quad (\text{A3})$$

using the relations

$$\frac{1}{W \pm i\epsilon - W'} = P \frac{1}{W - W'} \mp i\pi\delta(W - W').$$

We can easily see from Eq. (A2) that $I_{\pm}(\vec{q})$ depend

on the absolute value of \vec{q} ; namely, we get

$$I_{\pm}(\vec{q}) = I_{\pm}(-\vec{q}). \quad (\text{A4})$$

Further, if we take into account the symmetry property of the Green function, $G_{\Psi}(\vec{r}, \vec{r}') = G_{\Psi}(\vec{r}', \vec{r})$, we have

$$I_{-}(\vec{q})^* = I_{+}(-\vec{q}). \quad (\text{A5})$$

Then Eqs. (A4) and (A5) yield the following relation:

$$\begin{aligned} \text{Im} I_{\pm}(\vec{q}) &= [I_{\pm}(\vec{q}) - I_{\mp}(\vec{q})]/(2i) \\ &= \sum_{l_0 m_0} \langle n_0 l_0 m_0 | e^{-i\vec{q} \cdot \vec{r}} \text{Im} G_{W \pm i\epsilon}(\vec{r}, \vec{r}') \times e^{i\vec{q} \cdot \vec{r}'} | n_0 l_0 m_0 \rangle, \end{aligned} \quad (\text{A6})$$

where use has been made of the relation

$$G_{W+i\epsilon}(\vec{r}, \vec{r}') = [G_{W-i\epsilon}(\vec{r}, \vec{r}')]^*.$$

From Eqs. (A3) and (A6), we obtain

$$\begin{aligned} \sum_{l_0 m_0} \langle n_0 l_0 m_0 | e^{-i\vec{q} \cdot \vec{r}} \text{Im} G_{W \pm i\epsilon}(\vec{r}, \vec{r}') e^{i\vec{q} \cdot \vec{r}'} | n_0 l_0 m_0 \rangle \\ = \mp \pi \sum_{l_0 m_0} \int d\Omega |\langle E\Omega \pm | e^{i\vec{q} \cdot \vec{r}} | n_0 l_0 m_0 \rangle|^2. \end{aligned}$$

Further, using the relation for a negative real W' ,

$$\sum_{l_0 m_0} |n_0 l_0 m_0 \rangle \langle n_0 l_0 m_0| = \lim_{W' \rightarrow W_{n_0}} (W' - W_{n_0}) G_{W'}(\vec{r}, \vec{r}'),$$

we get Eq. (2.6).

*Work performed under the auspices of the U. S. Atomic Energy Commission.

† Visiting Scientist, 1972–1973. Permanent address: The University of Electron-Communications, Chofushi, Tokyo, Japan.

¹M. J. Seaton, Commun. Atom. and Mol. Phys. **2**, 37 (1970), and references therein.

²A. O. Barut and H. Kleinert, Phys. Rev. **160**, 1149 (1967).

³(a) G. C. McCoyd, S. N. Milford, and J. J. Wahl, Phys.

- Rev. 119, 149 (1960); (b) L. Fisher, S. N. Milford, and F. R. Pomilla, Phys. Rev. 119, 153 (1960); (c) S. N. Milford, J. J. Morrissey, and J. H. Scanlon, Phys. Rev. 120, 1715 (1960).
- ⁴K. Omidvar, Phys. Rev. 188, 140 (1969).
- ⁵(a) H. E. Saraph, Proc. Phys. Soc. Lond. 83, 763 (1964); (b) K. Omidvar and A. H. Khateeb, J. Phys. B 6, 341 (1973); (c) A. E. Kingston and J. E. Lauer, Proc. Phys. Soc. Lond. 87, 399 (1966); (d) 88, 597 (1967).
- ⁶I. L. Beigman, A. M. Urnov, and V. P. Shevel'ko, Zh. Eksp. Teor. Fiz. 58, 1825 (1970) [Sov. Phys.—JETP 31, 978 (1970)].
- ⁷K. Omidvar, Phys. Rev. 140, A26 (1965).
- ⁸K. Omidvar, Goddard Space Flight Center Report X-641-68-505, 1968 (unpublished).
- ⁹For example, A. E. Kingston, Proc. Phys. Soc. Lond. 86, 1279 (1965). See also Ref. 5(b).
- ¹⁰M. Inokuti and R. L. Platzman, in *Fourth International Conference on the Physics of Electronic and Atomic Collisions. Abstracts of Papers* (Science Bookcrafters, Hasting-on-Hudson, New York, 1965), p. 408.
- ¹¹(a) M. Matsuzawa, J. Chem. Phys. 55, 2685 (1971); (b) 58, 2674 (1973).
- ¹²G. Breit and H. A. Bethe, Phys. Rev. 93, 888 (1954).
- ¹³L. Hostler and R. H. Pratt, Phys. Rev. Lett. 10, 469 (1963).
- ¹⁴As for the definitions of the Whittaker functions W and M , for example, see I. S. Gradshteyn and I. M. Ryzhik, *Tables of Integrals, Series, and Products* (Academic, New York, 1965), p. 1059.
- ¹⁵For example, see Ref. 14, p. 1061, formula 9:231, 2, and p. 1062, formula 9.233, 1.
- ¹⁶(a) B. J. Laurenzi, Chem. Phys. Lett. 5, 3 (1970); see Eq. (13) in Appendix of this reference. (b) B. J. Laurenzi [private communication, which states $\cosh(\pi\nu)$ in Eq. (13) of Appendix in Ref. 16(a) is a typographical error and should be replaced with $\coth(\pi\nu)$].
- ¹⁷A. R. Holt, J. Phys. B 2, 1209 (1969).
- ¹⁸There are misprints in Eqs. (10) and (13) of Ref. 6. Equation (10) should read $A(q) = (48 nn')^{-1} \int_0^{\infty} e^{-iq(x-y)/2} \times (x^2 + 4xy + y^2) P_n P_{n'} dx dy$, and a factor of $\frac{1}{2}$ after the notation Re in the right-hand side of Eq. (13) should be deleted.
- ¹⁹H. Bethe, Ann. Phys. (Leipz.) 5, 325 (1930).
- ²⁰D. H. Menzel and C. L. Perkeris. Mon. Not. R. Astron. Soc. 96, 77 (1935).
- ²¹For more detailed results, see Argonne National Laboratory Radiological and Environmental Research Division Annual Report, ANL-8060, Pt. I, 1973 (unpublished).
- ²²M. Inokuti, Rev. Mod. Phys. 43, 297 (1971), p. 311.
- ²³See also Ref. 22, p. 307.
- ²⁴L. Vriens, *Case Studies in Atomic Collision Physics I*, edited by E. W. McDaniel and M. R. C. McDowell (North-Holland, Amsterdam, 1969), p. 337.
- ²⁵See also Ref. 22, p. 335.
- ²⁶For example, (a) M. R. Flannery, J. Phys. B 3, 1610 (1970); (b) I. C. Percival, J. Phys. B 6, 93 (1973).
- ²⁷J. D. Garcia, Phys. Rev. 159, 39 (1967).
- ²⁸V. Fock, Z. Phys. 98, 145 (1935).
- ²⁹V. S. Nikolaev and I. M. Kruglova, Phys. Lett. A 37, 315 (1971).
- ³⁰U. Fano, Phys. Rev. 95, 1198 (1954).
- ³¹L. C. Johnson, Phys. Rev. 155, 64 (1967).